JOURNAL OF VIROLOGY, Nov. 2006, p. 10652–10662 Vol. 80, No. 21
0022-538X/06/$08.00+0 doi:10.1128/JVI.01183-06

Integrity of Membrane Lipid Rafts Is Necessary for the Ordered Assembly and Release of Infectious Newcastle Disease Virus Particles

Jason P. Laliberte,[1] Lori W. McGinnes,[2] Mark E. Peeples,[3] and Trudy G. Morrison[1,2]*

Program in Immunology/Virology[1] and Department of Molecular Genetics and Microbiology,[2] University of Massachusetts Medical School, 55 Lake Avenue North, Worcester, Massachusetts 01655, and Columbus Children's Research Institute, Center for Vaccines and Immunity, The Ohio State University, Columbus, Ohio 43205[3]

Received 7 June 2006/Accepted 5 August 2006

Membrane lipid raft domains are thought to be sites of assembly for many enveloped viruses. The roles of both classical lipid rafts and lipid rafts associated with the membrane cytoskeleton in the assembly of Newcastle disease virus (NDV) were investigated. The lipid raft-associated proteins caveolin-1, flotillin-2, and actin were incorporated into virions, while the non-lipid raft-associated transferrin receptor was excluded. Kinetic analyses of the distribution of viral proteins in lipid rafts, as defined by detergent-resistant membranes (DRMs), in non-lipid raft membranes, and in virions showed an accumulation of HN, F, and NP viral proteins in lipid rafts early after synthesis. Subsequently, these proteins exited the DRMs and were recovered quantitatively in purified virions, while levels of these proteins in detergent-soluble cell fractions remained relatively constant. Cholesterol depletion of infected cells drastically altered the association of viral proteins with DRMs and resulted in an enhanced release of virus particles with reduced infectivity. Decreased infectivity was not due to effects on subsequent virus entry, since the extraction of cholesterol from intact virus did not significantly reduce infectivity. Particles released from cholesterol-depleted cells had very heterogeneous densities and altered ratios of NP and glycoproteins, demonstrating structural abnormalities which potentially contributed to their lowered infectivity. Taken together, these results indicate that lipid rafts, including cytoskeleton-associated lipid rafts, are sites of NDV assembly and that these domains are important for ordered assembly and release of infectious Newcastle disease virus particles.

Paramyxoviruses, such as Newcastle disease virus (NDV), are enveloped, negative-sense RNA viruses. NDV virions contain four main structural proteins, i.e., the nucleocapsid (NP), matrix (M), fusion (F), and hemagglutinin-neuraminidase (HN) proteins, as well as the polymerase complex of phosphoprotein (P) and the large (L) protein (19). Although many details of the paramyxovirus life cycle are well known, virion assembly and release are less well characterized. Specific viral protein-protein interactions are likely required for assembly, but they are incompletely characterized (46). Cellular proteins are necessary for the release of many enveloped viruses, including paramyxoviruses (35, 41), but their roles remain to be clarified fully. Membrane lipid raft domains are also thought to be important in virion assembly and release for several types of enveloped viruses (32); however, the role of these domains in paramyxovirus assembly and release is not well understood.

Membrane lipid raft domains have been implicated in the assembly and release of a wide variety of viruses, including human immunodeficiency (HIV), Ebola, Marburg, influenza, and measles viruses (reviewed in reference 32). Membrane lipid rafts are defined as cholesterol- and sphingolipid-rich microdomains in the exoplasmic leaflet of the cellular plasma membrane (42). The tight packing of cholesterol molecules among the saturated fatty acid tails of sphingolipids creates a local membrane organization, referred to as "liquid-ordered," which possesses properties different from those of the surrounding bulk plasma membrane (42). Specific proteins, such as raft-organizing, acylated, and glycosylphosphatidylinositol-anchored proteins, partition into these domains, resulting in their concentration into patches within the plasma membrane. Membrane lipid rafts function in membrane trafficking events and cell-cell attachment and serve as signal transduction platforms in many cell types (42).

Membrane lipid rafts are also thought to be sites of virus assembly and release, based primarily on two lines of reasoning. First, lipid raft-associated molecules are found in purified virions. For example, the ganglioside GM1, glycosylphosphatidylinositol-anchored Thy-1 and CD59 proteins, and caveolin-1 have all been detected variably in HIV, influenza virus, and several paramyxoviruses (4, 31, 34, 37). Second, viral proteins fractionate with detergent-resistant membranes (DRMs), a cell fraction that biochemically reflects lipid rafts (42). The Env glycoproteins of HIV type 1 (31) and murine leukemia virus (21) have been detected in DRMs. Both influenza HA (44) and NA (3) glycoproteins were found to be associated with DRMs. Among the paramyxovirus glycoproteins, the Sendai virus F and HN proteins (39), measles virus F protein (48), respiratory syncytial virus (RSV) F protein (14), RSV SH protein (36), and NDV F protein (6) have been associated with DRMs.

The peripheral membrane-associated matrix-like proteins of different types of enveloped viruses drive the release of virus and virus-like particles (41). These proteins also associate, directly or indirectly, with DRMs. The HIV Gag protein intrinsically associates with DRMs (31). However, the influenza

* Corresponding author. Mailing address: Department of Molecular Genetics and Microbiology, University of Massachusetts Medical School, 55 Lake Avenue North, Worcester, MA 01655. Phone: (508) 856-6592. Fax: (508) 856-5920. E-mail: trudy.morrison@umassmed.edu.

virus M1 protein targets to DRMs only when coexpressed with HA and NA glycoproteins (1). Similarly, the Sendai virus M protein stably associates with DRMs only when the F or HN protein is present (2), while the RSV M protein requires expression with the F protein for DRM association (14). In contrast, the measles virus M protein displays an innate affinity for DRMs in the absence of other viral proteins (48).

To explore the functional significance of paramyxovirus protein associations with membrane lipid rafts, the role of these domains in the assembly and release of Newcastle disease virus was characterized. As reported for other systems, NDV particles contained lipid raft-associated proteins but not a nonraft protein, and NDV proteins were found in DRMs. To extend these results, NDV proteins were first shown to be associated with a newly defined class of DRMs, those that are attached to the cortical membrane cytoskeleton (30). Second, a kinetic analysis of the NDV proteins' association and dissociation with DRMs and incorporation into virions suggested a direct relationship between DRM dissociation and virion release. Third, the perturbation of membrane lipid rafts by cholesterol depletion significantly stimulated the release of structurally abnormal and noninfectious virus particles. Taken together, these results suggest that the integrity and organization of cholesterol-rich membrane lipid rafts are critical for the ordered assembly and release of infectious Newcastle disease virus particles.

MATERIALS AND METHODS

Cells, virus, and reagents. East Lansing Line (ELL-0) avian fibroblasts from the American Type Culture Collection were maintained in Dulbecco's modified Eagle medium (DMEM) supplemented with penicillin-streptomycin and 10% fetal calf serum (FCS). NDV strain AV stocks were prepared by growth in eggs by standard protocols (25) under biosafety level 3 conditions. Methyl-β-cyclodextrin (mβCD; Sigma-Aldrich) was resuspended in DMEM. Lovastatin (Sigma-Aldrich) was prepared in H_2O and activated as described previously (8). Triton X-100 was purchased from Pierce Biotechnology.

Antibodies. Anti-caveolin-1 was obtained from Santa Cruz Biotechnology, anti-flotillin-2 was obtained from BD Transduction Labs, anti-transferrin receptor was obtained from Zymed Laboratories, and anti-actin was obtained from Sigma-Aldrich. Anti-NDV (26), anti-M (7), HN protein-specific anti-A (24), F protein-specific anti-HR1 (23), anti-HR2 (6), anti-F_{tail} (49), anti-F_2-96 (24), and anti-Fu1a (29) have been described previously.

Infections and radioactive labeling. ELL-0 cells seeded at approximately 6×10^5 cells per 35-mm plate were grown overnight and then infected with NDV at a multiplicity of infection of 10 in 0.25 ml of medium under biosafety level 3 conditions. After 45 min, 1 ml of medium was added, and monolayers were incubated for 5 to 8 h. For radioactive labeling, cells were radiolabeled at 6 h postinfection for 20 min (kinetic experiments) or 1 h (mβCD experiments) at 37°C in DMEM supplemented with 100 μCi of [^{35}S]methionine-cysteine per ml (New England Nuclear). At the end of the labeling period, cells were incubated with chase medium (DMEM supplemented with 0.1 mM cold methionine, with or without 10% FCS). At the end of each nonradioactive chase time point, culture supernatants were collected for virion purification on gradients and cells were harvested for isolation of DRMs as described below.

Virus purification. Culture supernatants were clarified by centrifugation at 5,000 rpm for 5 min, and then particles in the supernatant were subjected to sedimentation through 20% sucrose (wt/vol) to a 20 to 65% sucrose interface (24,000 rpm for 10 to 12 h at 4°C, using a Beckman SW50.1 rotor). For virion flotation, purified virus taken from 20 to 65% sucrose interface fractions was adjusted to ~60% sucrose (wt/vol) and used to overlay ~80% (1.24 g/cm^3) sucrose. The sucrose layer containing the virus was then overlaid with 1 ml 50% sucrose, 1 ml 38% sucrose, and 0.5 ml 10% sucrose in an SW50.1 tube. Samples were subjected to centrifugation at 100,000 × *g* for 18 h at 4°C. Fractions were collected from the bottom of the gradient (each fraction was 0.5 ml, except for the first fraction, which had a volume of 1 ml). For virion sedimentation, purified virus taken from 20 to 65% sucrose interface fractions was adjusted to ~10% sucrose (wt/vol) and used to overlay a 20 to 65% continuous sucrose gradient. Samples were subjected to centrifugation at 100,000 × *g* for 18 h at 4°C. Fractions (0.5 ml) were collected from the bottom of the gradient. All fractions were made 1% with respect to Triton X-100 and 0.5% with respect to sodium deoxycholate. Viral proteins were immunoprecipitated and resolved by sodium dodecyl sulfate-polyacrylamide gel electrophoresis (SDS-PAGE) as described below. The densities of all sucrose fractions were measured using a refractometer and are indicated in g/cm^3.

Preparation of protein-containing samples for SDS-PAGE and Western analysis. For cell extracts, ELL-0 cell monolayers were washed with phosphate-buffered saline (PBS) and lysed in TNE (25 mM Tris-HCl, pH 7.4, 150 mM $NaCl_2$, and 5 mM EDTA) containing 1% Triton X-100, 0.5% sodium deoxycholate, and 2.5 mg/ml of *N*-ethylmaleimide. For gradient fractions, viral proteins were immunoprecipitated using a cocktail of antibodies (anti-NDV, anti-M, anti-A, anti-Fu1a, anti-F_2-96, anti-HR1, anti-HR2, and anti-F_{tail} antibodies). Antibody complexes were precipitated with pansorbin cells (Calbiochem) and washed three times with PBS containing 0.4% SDS. All protein-containing samples were diluted in 2× sample buffer (125 mM Tris-HCl, pH 6.8, 2% SDS, 10% glycerol), with or without 0.7 M β-mercaptoethanol, and boiled for 2 to 5 min prior to being loaded into 8% polyacrylamide gels. Following electrophoresis, gels were transferred to Immobilon-P (Millipore Corporation) membranes for Western blot analysis. The membranes were blocked for 2 to 4 h at 4°C in PBS containing 0.5% Tween 20 and 10% nonfat milk, washed with PBS-Tween 20, and incubated for 1 h at room temperature with primary antibody in PBS-Tween 20. Membranes were then washed, incubated for 1 h at room temperature with secondary antibody (goat anti-rabbit immunoglobulin coupled to horseradish peroxidase [Amersham Biosciences]) in PBS-Tween 20, and then washed in PBS-Tween 20 prior to detection with the ECL Western blotting detection reagent system (Amersham Biosciences). Polyacrylamide gels containing radiolabeled proteins were fixed in acetic acid, treated with 2,5-diphenyloxazole (Sigma-Aldrich), dried for 1.5 to 2 h, and placed on X-ray film at −80°C. Signals in autoradiographs were quantified using a Fluor-S phosphorimager (Bio-Rad).

Isolation of detergent-resistant membranes. Cell monolayers were washed once in ice-cold PBS, and cells were lysed in ice-cold TNE containing 1% Triton X-100 and 2.5 mg/ml *N*-ethylmaleimide. Lysates were incubated on ice at 4°C for 30 min and then subjected to centrifugation for 15 s at 5,000 rpm. The supernatants were kept on ice for an additional 30 min, mixed with ice-cold sucrose to produce a final sucrose density of ~60% (wt/vol), placed on top of 0.25 ml ~80% (1.24 g/cm^3) sucrose in an SW50.1 tube, and overlaid with 1 ml 45% sucrose, 0.5 ml 43% sucrose, 0.5 ml 38% sucrose, 0.5 ml 32% sucrose, 0.5 ml 28% sucrose, 0.5 ml 18% sucrose, and 0.5 ml 5% sucrose, all dissolved in TNE. Samples were subjected to centrifugation at 100,000 × *g* for 18 h at 4°C. Fractions were collected from the bottom of the gradient (each fraction was 0.25 ml, except for the second fraction, which had a volume of 1 ml). Proteins in each fraction were resolved by 8% SDS-PAGE and detected by Western analysis with the appropriate primary and secondary antibodies. An uninfected cell plate with comparable cell numbers was used for the detection of host cell proteins. After centrifugation, the densities of all sucrose fractions were measured using a refractometer and are indicated in g/cm^3.

Determination of cholesterol levels. Cholesterol levels in ELL-0 cell monolayers and virion envelopes were determined using an Amplex Red cholesterol assay kit (Molecular Probes) according to the manufacturer's protocol.

Extraction of cholesterol. ELL-0 cells seeded on 35-mm plates were infected and radiolabeled for 1 h as described above. At the end of the labeling period, monolayers were incubated with chase medium (DMEM supplemented with 0.1 mM cold methionine only) for 1 h. Cells were then either left untreated or treated with increasing concentrations of methyl-β-cyclodextrin and 4 μg/ml lovastatin for 1 h in DMEM supplemented with 0.1 mM cold methionine only at 37°C. A final 4-h nonradioactive chase was performed in the absence of mβCD but in the presence of lovastatin. Culture supernatants were then collected for virion purification, and cells were harvested for the isolation of DRMs. Uninfected and unlabeled cells were treated with mβCD in an identical protocol.

Actin and surface GM1 staining and visualization. ELL-0 cells were grown to confluence on glass coverslips in 35-mm plates. Cells were then left untreated or treated with 4 μg/ml lovastatin alone, 5 mM mβCD and 4 μg/ml lovastatin, or 10 mM mβCD and 4 μg/ml lovastatin for 1 h, followed by a 1-h recovery in DMEM only. Cells were then washed twice with ice-cold IF buffer (PBS containing 1% bovine serum albumin, 0.02% sodium azide, and 5 mM $CaCl_2$), fixed with 2% paraformaldehyde for 10 min on ice, and blocked with IF buffer overnight at 4°C. Cells processed for actin visualization were permeabilized with IF buffer containing 0.05% Triton X-100 for 20 min on ice at 4°C prior to the overnight block in IF buffer. Cells were then incubated for 1 h at 4°C in IF buffer containing Alexa fluor 488-conjugated cholera toxin subunit B (Molecular Probes) or Alexa fluor 568-conjugated phalloidin (Molecular Probes), washed three times with

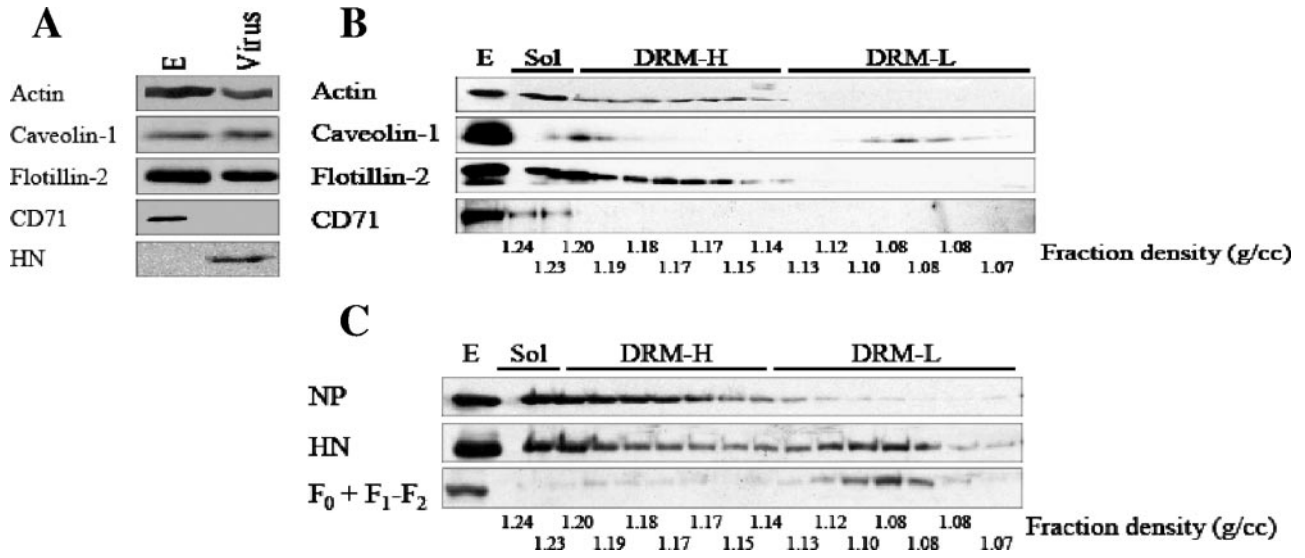

FIG. 1. Preferential assembly and release of NDV from lipid raft domains. (A) Proteins in gradient-purified, egg-grown NDV (virus) and in avian ELL-0 cell extracts (E) were resolved by SDS-PAGE and detected by Western analysis with antibodies directed against the indicated proteins. (B) DRMs in extracts of uninfected avian ELL-0 cells were isolated by flotation in sucrose gradients, as described in Materials and Methods. Proteins present in DRM gradient fractions were probed by Western analysis for the indicated proteins. (C) DRMs in extracts of NDV-infected avian ELL-0 cells were isolated by flotation in sucrose gradients, and proteins present in the gradient fractions were probed with the following antibodies specific for NDV proteins: anti-NDV (NP), anti-A (HN), and anti-HR2 (F_0 + F_1-F_2). Each lane contained 12% of the corresponding gradient fraction, except for fraction 2, which contained 3% of the total. The density of each gradient fraction is indicated in g/cm^3. E, total cellular extract; Sol, detergent-soluble gradient fractions; DRM-H, high-density DRM gradient fractions; DRM-L, low-density DRM gradient fractions; NP, nucleocapsid protein; HN, hemagglutinin-neuraminidase protein; F_0, uncleaved fusion protein; F_1-F_2, disulfide-linked, cleaved fusion protein.

ice-cold IF buffer, and incubated for 20 min on ice with IF buffer containing Hoechst nuclear stain (Molecular Probes). Cells were washed twice with ice-cold IF buffer and mounted on slides, using Vectashield mounting medium (Vector Laboratories), for fluorescence microscopy. Fluorescence images were acquired using a Nikon fluorescence microscope and Openlab software.

Viral plaque assay. Purified virus, taken from 20 to 65% sucrose interface or density gradient flotation fractions, was serially diluted in Ca^{2+}-rich medium and allowed to adsorb to confluent monolayers of ELL-0 cells for 45 min. Agar diluted to 1% in DMEM and supplemented with nonessential amino acids, vitamins, penicillin-streptomycin, sodium bicarbonate, and 10% FCS was then placed over the monolayers. After 48 h of incubation, plaques were counted. To normalize infectivity to the levels of NP found in virus particles, the calculated PFU/ml value was divided by the Fluor-S value obtained for NP found in released virions for the corresponding sample.

Negative staining of particles for transmission electron microscopy. Virions were purified to 20 to 65% sucrose interface fractions as described above. Particles contained in interface fractions were then pelleted (40,000 rpm for 10 to 12 h at 4°C in a Beckman SW50.1 rotor) and resuspended in TNE containing 2.5% glutaraldehyde. The fixed samples were then spread on freshly prepared carbon-stabilized Formvar support films (either copper or gold grids). After 30 s, the grids were washed twice with TNE buffer. The grids were negatively stained with 1% uranyl acetate in water.

Extraction of cholesterol from NDV particles. Egg-grown, purified virions were mixed with Ca^{2+}-rich DMEM or with increasing concentrations of mβCD in Ca^{2+}-rich DMEM and incubated for 1 h at 37°C. One percent of the treated virus was serially diluted in Ca^{2+}-rich DMEM and used for viral plaque assays as described above. The remainder of the virus was purified away from mβCD-cholesterol complexes by sedimentation through 20% sucrose. Virion-associated cholesterol from pelleted virions was released by treatment of virus with 1% Triton X-100 and 0.5% sodium deoxycholate and measured using an Amplex Red cholesterol assay kit.

RESULTS

Incorporation of cellular lipid raft- and non-lipid-raft-associated proteins into NDV particles. To determine if membrane lipid rafts serve as preferential platforms for the assembly and release of NDV, proteins in purified virions were probed by Western analysis for the presence of both lipid raft-associated and non-lipid-raft membrane proteins. The lipid raft-associated proteins caveolin-1 (27) and flotillin-2 (38) were detected in avian ELL-0 cells and also in virus particles (Fig. 1A). However, the non-raft-associated plasma membrane transferrin receptor CD71 (12) was not found in virions, although it was detected in avian cells (Fig. 1A). These results are consistent with membrane lipid rafts being sites of NDV assembly and release.

Association of NDV viral proteins with detergent-resistant membranes. If virus assembly occurs in membrane lipid rafts, then viral proteins should be associated with these domains in infected cells. Since DRMs are thought to experimentally reflect lipid rafts, the association of viral proteins with these membranes from infected cells was characterized after cell lysis with cold Triton X-100. For this analysis, a class of DRMs which were only recently recognized was included. Luna and colleagues (30) characterized a class of DRMs with higher buoyant densities (1.20 to 1.14 g/cm^3) than those of classical DRMs, which have densities of 1.13 to 1.08 g/cm^3. The high-density detergent-resistant membranes were termed DRM-H, while classical DRMs were termed DRM-L. The increased density of DRM-H is due to their association with the underlying membrane cytoskeleton, as illustrated by the presence of actin in the corresponding gradient fractions (Fig. 1B) (30). DRM-H also contain flotillin-2, while DRM-L preferentially possess caveolin-1 (Fig. 1B) (30). Nonraft membrane material was effectively solubilized, as the nonraft transferrin receptor

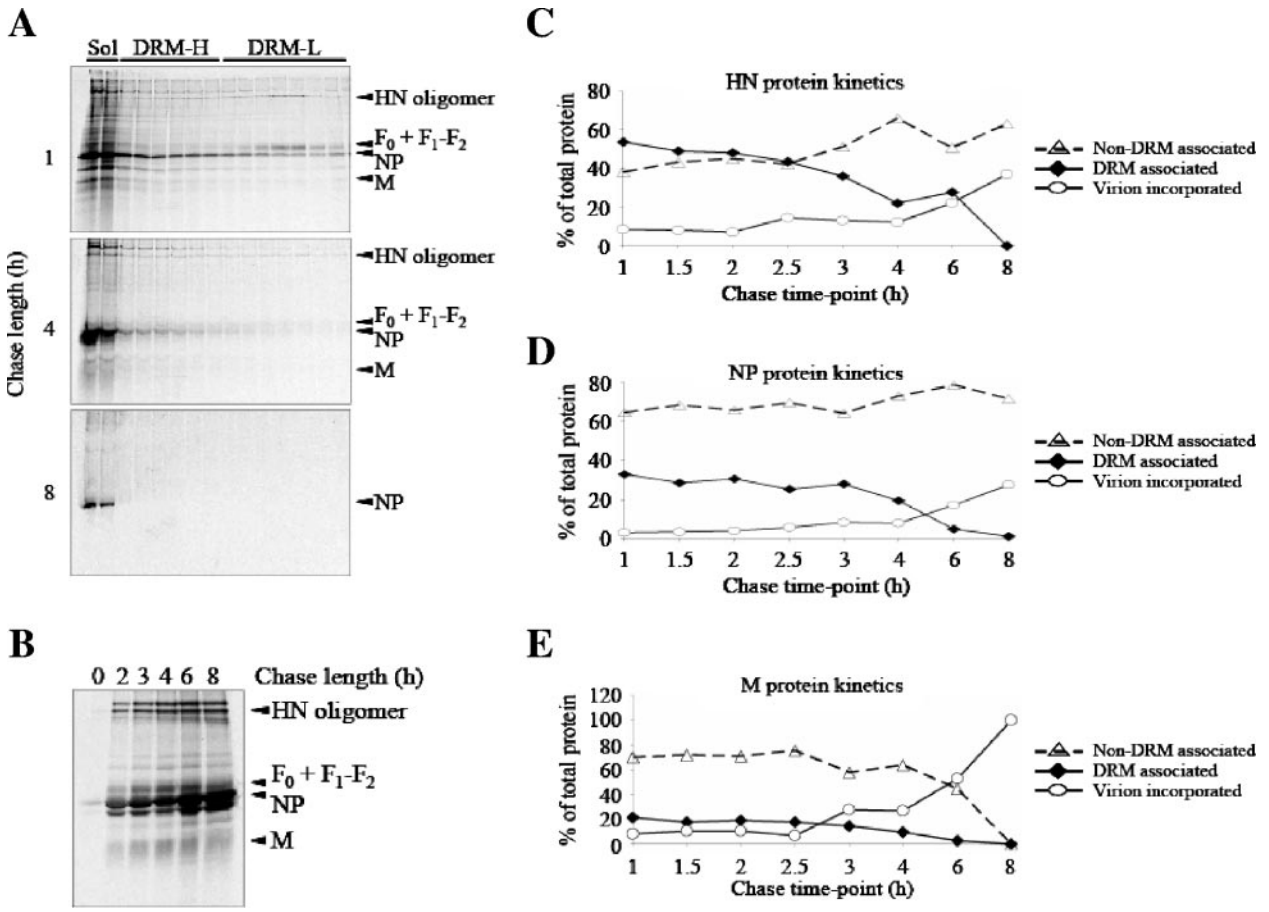

FIG. 2. Kinetics of pulse-labeled viral protein dissociation from DRMs and virion incorporation. Monolayers of NDV-infected avian ELL-0 cells were pulse-labeled with [^{35}-S]methionine-cysteine and then subjected to nonradioactive chases of 0 to 8 h, as described in Materials and Methods. (A) DRMs in cell extracts were isolated by flotation in sucrose gradients, and proteins present in each gradient fraction were resolved by polyacrylamide gel electrophoresis and detected by autoradiography. The images shown are representative autoradiographs derived from cells subjected to nonradioactive chases of 1, 4, or 8 h. Each lane contained 12% of the corresponding gradient fraction, except for fraction 2, which contained 3% of the total. (B) Radiolabeled proteins in virions purified from supernatants of cells subjected to nonradioactive chases were resolved by polyacrylamide gel electrophoresis and detected by autoradiography. The image shown is a representative autoradiograph of radiolabeled viral proteins in virions released from cells at different nonradioactive chase times, as indicated at the top of the panel. Each lane contained 20% of the total virions isolated. (C to E) Amounts of radiolabeled HN protein (C), NP protein (D), and M protein (E) in detergent-soluble/non-DRM gradient fractions, total DRM (DRM-H plus DRM-L) gradient fractions, and virions after different nonradioactive chase times (shown at the bottom of each panel) were determined by densitometry of autoradiographs of polyacrylamide gels such as those shown in panels A and B. Results are averages for three separate experiments.

protein remained in the bottom of the gradient and did not float up into the gradient with either class of DRMs (Fig. 1B).

The HN protein, F protein, and NP protein could be detected in both DRM-H and DRM-L (37%, 84%, and 33% of total HN, F, and NP protein, respectively) (Fig. 1C). The majority of DRM-associated NP protein and most of the HN protein was found in DRM-H. The detection of significant amounts of the major structural NDV proteins in detergent-resistant membranes further suggested that membrane lipid rafts may serve as sites of virus assembly and release.

Kinetics of viral protein DRM dissociation and virion incorporation. If membrane lipid rafts serve as platforms for virus assembly, then viral proteins should transit through lipid rafts prior to assembly into virions. Thus, the kinetics of DRM dissociation and virion incorporation of the HN, F, NP, and M proteins were analyzed, utilizing an ^{35}S pulse-chase labeling protocol. At each nonradioactive chase time point, culture supernatants were collected for virion purification, while cell monolayers were harvested for DRM isolation in sucrose gradients. Representative autoradiographs of the sucrose gradient distributions of radiolabeled proteins for three different chase time points are shown in Fig. 2A. Radiolabeled proteins recovered in virions at different chase time points are shown in Fig. 2B. After short chases, the HN and F glycoproteins fractionated primarily with DRM-L, while the majority of DRM-associated NP and M proteins were found in DRM-H. Levels of all viral proteins in both classes of DRMs were reduced at later chase times, and virtually no labeled viral protein could be found in either class of DRMs after 8 h of chase.

Quantification of the amounts of HN protein and NP protein in total DRMs (DRM-H and DRM-L) and in detergent-soluble fractions at different chase times is shown in Fig. 2C

and D. After 1 hour of chase, 55% of total HN protein was found in DRM fractions, while 35% of total NP was in DRM fractions. With increasing chase times, a decline in the amounts of both HN protein and NP in DRMs was observed. Nearly all of the radiolabeled HN protein and NP found in DRMs in early chases was recovered in virions purified by 8 h of nonradioactive chase.

The HN protein and NP not associated with DRMs (i.e., detergent-soluble material which remained in the bottom of the gradient in fractions 1 and 2) did not contribute significantly to the HN protein and NP packaged into released virus particles, since the amounts of detergent-soluble HN protein and NP remained relatively constant during the course of the experiment. However, a small amount of HN protein (approximately 15% of total HN protein) was found with detergent-soluble material at 4 h of nonradioactive chase and then recovered in virions. This result suggests that a transient association of HN protein with detergent-soluble membranes just prior to budding may have occurred. Similar kinetics for DRM dissociation and virion incorporation to those for NP and HN protein were seen for the F protein (illustrated in Fig. 3C). Thus, the disappearance of HN, F, and NP proteins from DRMs coincides with their appearance in virus particles, a result that is consistent with the proposal that viral proteins are packaged into virus particles at cholesterol-rich membrane lipid raft domains.

In contrast, the majority of M protein was detected in detergent-soluble fractions of the gradient throughout the pulse-chase protocol (Fig. 2E). The amounts of M protein associated with either class of DRMs during the nonradioactive chase were minimal in comparison to the levels of detergent-soluble M protein. Furthermore, the amounts of M protein found in DRMs were significantly less than those recovered in virions. This result may indicate that the M protein dissociates from DRMs during cell lysis or that it is packaged into virions from cytoplasmic pools. Alternatively, the M protein may associate transiently with DRMs prior to incorporation into virions.

Kinetics of protein dissociation from DRM-H and DRM-L. To determine if assembly occurred preferentially from DRM-H or DRM-L, the amounts of HN, NP, and F proteins in each class of DRMs during the chase were analyzed (Fig. 3). At early chase times, the HN and F glycoproteins (Fig. 3A and C, respectively) were found in both DRM-H and DRM-L, although both proteins were associated preferentially with DRM-L. In contrast, DRM-associated NP primarily associated with DRM-H during early chase times (Fig. 3B). The kinetics of loss of the HN and F proteins as well as NP from both DRM-H and DRM-L were similar. These results suggest that both classes of DRMs participate in the incorporation of HN, F, and NP proteins into virus particles.

Effects of cholesterol extraction on DRMs. If the virus is assembled in membrane lipid rafts, then a perturbation of raft integrity may affect that assembly. The integrity of membrane lipid rafts was disrupted by utilizing the cholesterol-extracting agent mβCD (17, 40, 42). To accomplish cholesterol extraction, cells were treated for 1 hour with increasing concentrations of mβCD in the presence of lovastatin, which inhibits the synthesis of endogenous cholesterol (16). Cells were then further incubated for either 1 or 4 hours in cholesterol- and serum-free medium in the presence of lovastatin only. After 1 hour of incubation, the total cellular levels of cholesterol in cells incubated with lovastatin alone were reduced by 60%, while cholesterol levels in cells treated with both lovastatin and increasing concentrations of mβCD were reduced up to 77% (Table 1). After 4 h of incubation in cholesterol- and serum-free medium, cholesterol levels in mβCD-treated cells remained at low levels (Table 1).

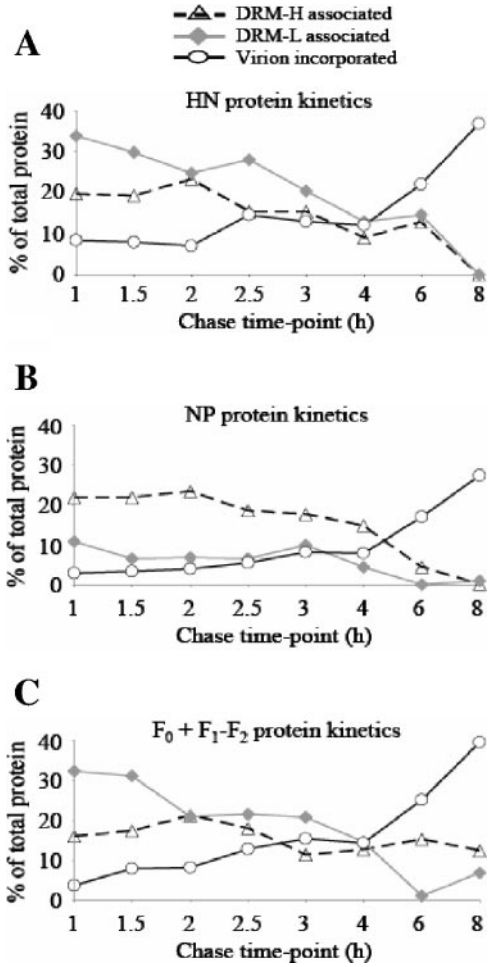

FIG. 3. Kinetics of viral protein dissociation from DRM-H and DRM-L. Amounts of radiolabeled HN (A), NP (B), and F (C) proteins in DRM-H and DRM-L gradient fractions as well as in purified virions at the indicated nonradioactive chase times were determined as described in the legend to Fig. 2. Gradient fractions corresponding to DRM-H and DRM-L were defined in the legends to Fig. 1 and 2.

One hour of treatment of cells with lovastatin alone or with increasing concentrations of mβCD and lovastatin had no effect on the cell number (data not shown). However, treatment of uninfected cells with mβCD significantly decreased the levels of detergent-resistant, lipid raft-associated proteins. After cholesterol extraction, caveolin-1 was found exclusively in the detergent-soluble gradient fractions, while the levels of DRM-H-associated actin were significantly reduced (Fig. 4A). Furthermore, the distribution of the glycolipid raft marker ganglioside GM1 on the surfaces of uninfected cells was significantly altered. In untreated cells, GM1 staining was relatively diffuse over the cell surface (Fig. 4B). However, upon treatment with

TABLE 1. Residual cholesterol in mβCD-treated avian ELL-0 cells

mβCD treatment (mM)[a]	Residual cholesterol			
	1 h posttreatment		4 h posttreatment	
	Amt (μg)	% of that in untreated cells	Amt (μg)	% of that in untreated cells
0	57.2 ± 10.7	100.0 ± 18.7	11.3 ± 2.5	100.0 ± 21.8
0 (+lovastatin)	22.7 ± 2.5	39.7 ± 4.3	5.3 ± 5.9	47.0 ± 52.4
2 (+lovastatin)	21.5 ± 2.9	37.6 ± 5.1	7.1 ± 3.2	62.4 ± 28.4
5 (+lovastatin)	16.7 ± 2.0	29.2 ± 3.5	6.6 ± 3.0	58.4 ± 26.6
7.5 (+lovastatin)	14.8 ± 1.7	25.9 ± 3.0	5.3 ± 2.9	47.1 ± 25.4
10 (+lovastatin)	13.3 ± 1.3	23.3 ± 2.3	4.8 ± 3.2	41.9 ± 28.3

[a] Uninfected avian ELL-0 cell monolayers were treated as indicated for 1 h at 37°C. A recovery time of 1 h or 4 h consisted of incubation of treated cells in DMEM only at 37°C. Cells were then subjected to cholesterol quantification as described in Materials and Methods. Data are means ± standard deviations.

mβCD, distinct foci or patches enriched in GM1 formed on the cell surface (Fig. 4B). This result was consistent with those reported by Hao et al. (11) following cholesterol extraction. The cellular distribution of actin in uninfected cells was also significantly altered upon cholesterol depletion (Fig. 4C).

After mβCD treatment of infected cells, the vast majority of NP, M, HN, and F proteins were found in detergent-soluble gradient fractions, with some residual glycoprotein material detected in DRM-H gradient fractions (Fig. 5A). Thus, treatment of cells with mβCD disrupts the association of raft proteins with DRMs, alters the distribution of actin and surface ganglioside GM1, and disrupts or alters the association of viral proteins with DRMs.

Effects of cholesterol extraction on virus release. To analyze the effects of mβCD on virus release, infected cells were ^{35}S radiolabeled at 6 h postinfection for 1 hour, followed by a 1-hour nonradioactive chase to allow transport of radiolabeled viral proteins to assembly sites. Cell monolayers were then incubated with various concentrations of mβCD for 1 hour in cholesterol- and serum-free medium and in combination with lovastatin. Cells were then incubated for a final 4-h nonradioactive chase in the absence of mβCD but in the presence of lovastatin. Virus particles were purified from culture supernatants, and the radiolabeled proteins present are shown in Fig. 5B. Based upon the quantification of radiolabeled NP recovered from purified virus, particle release was enhanced approximately twofold with mβCD cell treatment (Fig. 5C). However, particles released from untreated and mβCD-treated cells contained similar levels of M and F proteins and marginally smaller amounts of HN protein (Fig. 5B). These results suggested that particles released from cholesterol-extracted cells may be structurally abnormal.

Particles released from mβCD-treated cells are structurally abnormal, with reduced infectivity. To determine if virus particles released from mβCD-treated cells possessed an intact lipid envelope, the sensitivities of the NP and M core proteins to proteinase K were determined. Both proteins in cell extracts were digested with small amounts of proteinase K (Fig. 6A). In contrast, the NP and M proteins in virions released from untreated cells were resistant, reflecting their protection by the virion membrane. Similarly, the M protein and most of the NP protein in particles released from mβCD-treated cells were resistant to protease digestion, indicating that these particles

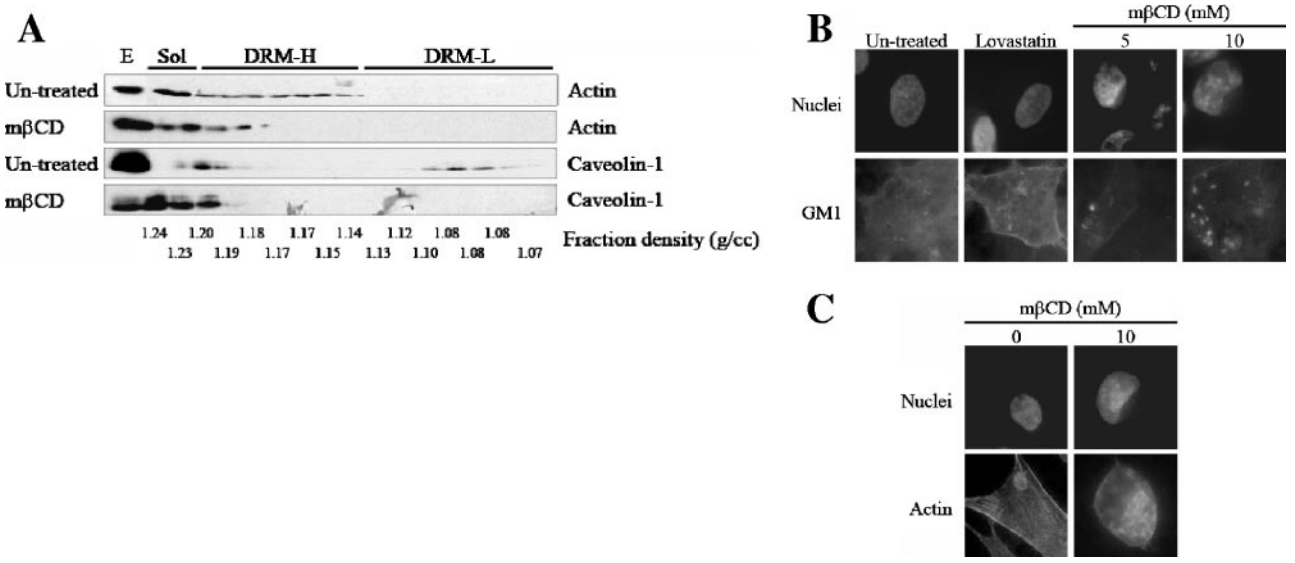

FIG. 4. Effects of cholesterol depletion on detection of lipid rafts. (A) Uninfected cells were left untreated or incubated with 10 mM mβCD and lovastatin as described in Materials and Methods. DRMs in extracts were isolated by flotation in sucrose gradients. Actin and caveolin-1 present in each gradient fraction were detected by Western analysis as described in the legend to Fig. 1. (B) Surface distribution of ganglioside GM1, as visualized by fluorescence microscopy. Uninfected cells were left untreated or treated with lovastatin alone (lovastatin), 5 mM mβCD and lovastatin (5 mM mβCD), or 10 mM mβCD and lovastatin (10 mM mβCD) for 1 h, followed by a 1-h incubation in DMEM. Nuclei are visualized in the top panels, while surface GM1 on the same cells, visualized as described in Materials and Methods, is shown in the bottom panels. (C) Distribution of actin, as visualized by fluorescence microscopy. Uninfected cells were left untreated or treated with 10 mM mβCD and lovastatin (10 mM mβCD) for 1 h, followed by a 1-h incubation in DMEM. Nuclei are visualized in the top panels, while actin in the same cells, visualized as described in Materials and Methods, is shown in the bottom panels.

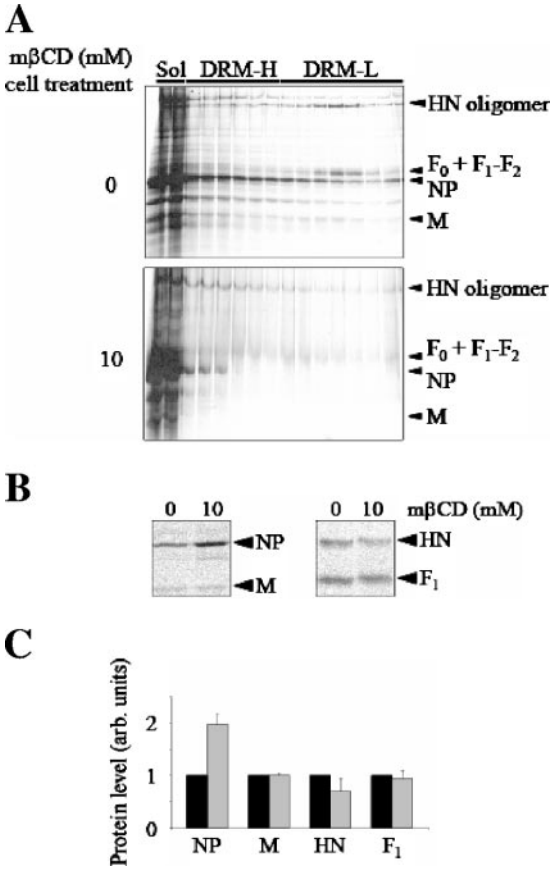

FIG. 5. Effects of cholesterol depletion on infected cell DRMs and virus release. Infected cells were radioactively labeled in a pulse-chase protocol in the absence or presence of 10 mM mβCD and lovastatin, as described in Materials and Methods. (A) Representative autoradiographs of DRM gradient distribution for radiolabeled viral proteins derived from untreated cells (top) or cholesterol-extracted cells (bottom) 1 h following the end of treatment. (B) Virions were isolated from 2×10^6 radioactively labeled cells either left untreated or treated with 10 mM mβCD. Proteins present in purified virions were immunoprecipitated using a cocktail of antibodies specific for the M and NP proteins (left panel) or the HN and F proteins (right panel). Excess antibody was used to ensure the precipitation of all virion proteins. (C) Amounts of HN, F, NP, and M proteins present in purified virions, detected as described above. Comparable experiments were quantified by densitometry, and the amount of each protein is given relative to the amount detected in virions from untreated cells. Black bars, untreated cells; gray bars, 10 mM mβCD-treated cells. Arb. units, arbitrary units.

were membrane enclosed and were not released RNP structures (Fig. 6A).

The observation that NP and M proteins were associated with lipids was also shown by their flotation in sucrose gradients (Fig. 6B). However, in contrast to virions from untreated cells, which had homogeneous densities of 1.18 to 1.16 g/cm^3 in sucrose, particles released from 5 mM and, particularly, 10 mM mβCD-treated cells had heterogeneous densities ranging from 1.23 to 1.12 g/cm^3 (Fig. 6B).

In contrast, sucrose gradient sedimentation of particles from untreated and mβCD-treated cells showed no difference in sedimentation. Radiolabeled particles released from mβCD-treated cells were present in the same fractions (5 to 7) of the sedimentation gradient as particles released from untreated cells (Fig. 6C). This result suggests that particles released from cholesterol-extracted cells had a size and shape similar to those of virus released from untreated cells but had altered protein-to-lipid ratios.

The infectivity of particles released from mβCD-treated cells, as determined by plaque assay, was decreased approximately 1 log (PFU/ml) compared to that of particles released from the same number of untreated cells (Fig. 6D). When virus titers were normalized to levels of NP, there was an even greater decrease in particle infectivity (Fig. 6D). To determine the infectivity of virions released from mβCD-treated cells that had a normal particle density, the infectivities of particles in individual fractions of gradients similar to those shown in Fig. 6B were determined. The peak infectivity of virions from untreated cells was found in fractions 4 to 6 (Fig. 6E). Particles released from 10 mM mβCD-treated cells possessing either normal (primarily fractions 5 and 6) or abnormal (fractions 4, 7, and 8) particle densities exhibited decreased infectivity compared to that of the control virus (Fig. 6E). Upon negative staining and analysis by transmission electron microscopy, particles released from untreated cells were visibly homogeneous in size and were spherical (Fig. 6F, panels i and ii). However, particles released from mβCD-treated cells were heterogeneous in size and shape (Fig. 6F, panels iii and iv). Interestingly, particles released from mβCD-treated cells tended to self-associate/aggregate (Fig. 6F, panel v). Thus, particles released from mβCD-treated cells are structurally abnormal, with significantly reduced infectivity.

Effect of cholesterol extraction of virions on infectivity. A direct measurement of cholesterol in particles released from untreated or 10 mM mβCD-treated cells revealed an approximately 37% reduction in cholesterol in particles released from mβCD-treated cells (data not shown). Since the decreased infectivity observed in Fig. 6 could be due to low cholesterol levels in the virion membrane, the effect of cholesterol depletion of virions on infectivity was determined. Egg-grown virus was depleted of cholesterol by incubation with increasing concentrations of mβCD. Incubation with 2 mM mβCD removed approximately 70% of the virion-associated cholesterol, while a higher concentration of mβCD removed approximately 90% (Fig. 7A). However, no significant decrease in infectivity was observed for any of the mβCD treatments (Fig. 7B). These results suggest that the presence of cholesterol in the virus envelope is not important for the infectivity of NDV particles and that its reduction in particles released from mβCD-treated cells cannot account for the reduced infectivity of these particles.

DISCUSSION

Membrane lipid rafts have been implicated in the assembly and release of many types of enveloped viruses, although the precise roles of these domains remain obscure. The incorporation of host cell lipid raft-associated proteins into the envelopes of viruses is indicative of preferential budding from these domains. Indeed, purified NDV particles contain lipid raft-associated caveolin and flotillin but do not contain detectable levels of a nonraft plasma membrane protein, the transferrin receptor. The presence of viral proteins in detergent-resistant membranes, a cell fraction that reflects lipid rafts (42), is also invoked as evidence for a role of lipid rafts in virus assembly

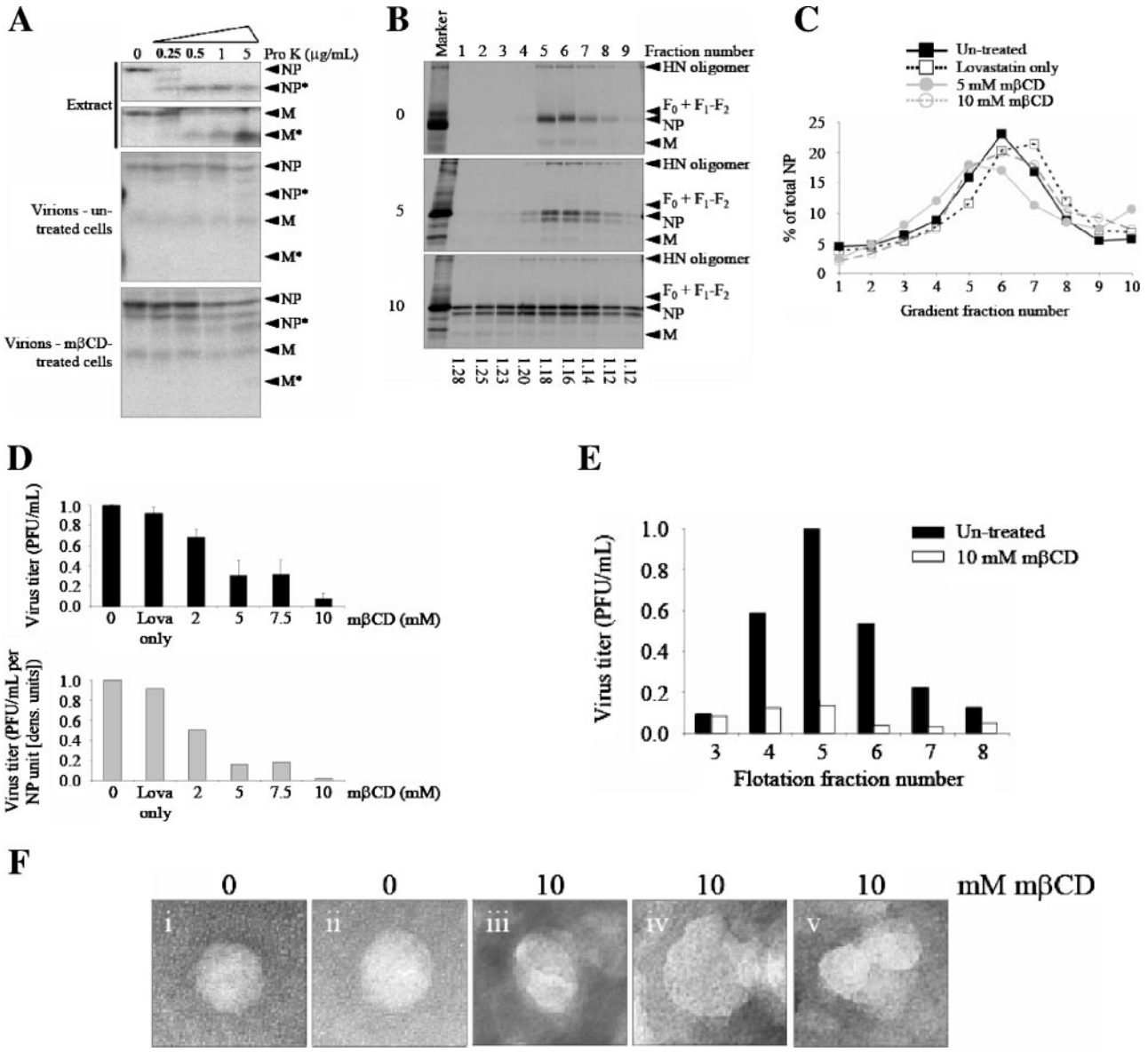

FIG. 6. Properties of virus particles released from mβCD-treated cells. (A) Protease resistance of virion-associated proteins. Cellular extracts containing radiolabeled viral proteins or gradient-purified virions released from untreated or 10 mM mβCD-treated cells were incubated with the indicated amounts of proteinase K for 30 min on ice. Reactions were stopped by the addition of 0.1 mM phenylmethylsulfonyl fluoride, particles were lysed, and viral proteins were immunoprecipitated and resolved in polyacrylamide gels. NP, nucleocapsid protein; NP*, NP cleavage product; M, matrix protein; M*, M cleavage product. (B) Sucrose density flotation gradient analysis of virions. Purified virions released from untreated or 5 mM mβCD- or 10 mM mβCD-treated cells were subjected to sucrose density flotation as outlined in Material and Methods. Viral proteins in individual gradient fractions were immunoprecipitated and resolved by SDS-PAGE. Gradient fraction numbers are indicated at the top, and fraction densities are displayed in g/cm^3 at the bottom. (C) Sucrose gradient sedimentation analysis of virions. Purified virions released from untreated, lovastatin-treated, or 5 mM mβCD- or 10 mM mβCD-treated cells were subjected to sedimentation in continuous sucrose gradients as outlined in Material and Methods. Viral proteins in individual gradient fractions were immunoprecipitated and resolved by SDS-PAGE. The level of NP in each gradient fraction was quantified and expressed as the percentage of total NP in each gradient. Gradient fraction numbers are indicated on the *x* axis. (D) Infectivity, determined by plaque assay, of purified virions released from untreated cells or cells treated with various concentrations of mβCD. 0, no treatment; Lova only, lovastatin-treated cells. Absolute infectivity (PFU/ml released from 2×10^6 cells) is shown in the top graph (black bars), and infectivity normalized to the level of NP protein quantified in the corresponding virions is shown in the bottom graph (gray bars). Infectivity is shown relative to the value obtained for particles released from untreated cells, which was set to 1. (E) Infectivity of viruses in the different fractions of sucrose flotation gradients shown in panel B. The infectivity in individual gradient fractions was determined by plaque assay, and virus titers are indicated in PFU/ml. Infectivity is shown relative to the value obtained for particles released from the same number of untreated cells, which was set to 1. Black bars, untreated cells; white bars, 10 mM mβCD-treated cells. Flotation gradient fraction numbers are indicated on the *x* axis. (F) Negative staining and transmission electron microscopy of particles released from untreated (panels i and ii) and mβCD-treated (panels iii, iv, and v) cells. Magnification, ×35,000.

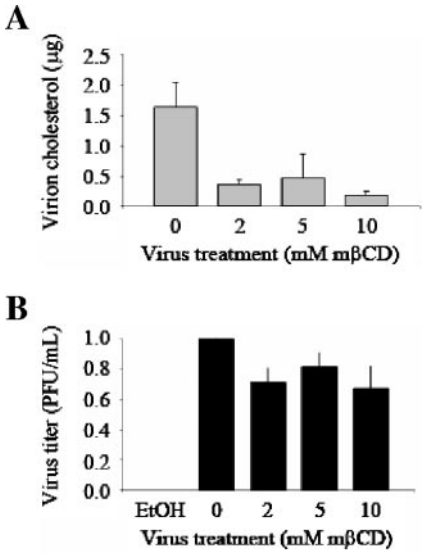

FIG. 7. Effect of virion cholesterol extraction on infectivity. Gradient-purified, egg-grown virus was depleted of cholesterol with 2, 5, and 10 mM mβCD for 1 h at 37°C and then repurified, and virion-associated cholesterol in untreated and treated virus was measured as described in Materials and Methods. (A) Residual cholesterol in virions following treatment. (B) Infectivity of untreated and mβCD-treated virus, as determined by viral plaque assay. Infectivity is shown relative to the value obtained for untreated particles, which was set to 1. EtOH, ethanol-treated control virus.

(reviewed in reference 32). At steady state, significant amounts of NDV proteins can be found in DRMs isolated from infected cells. Taken together, these results suggest that, similar to many enveloped viruses, NDV assembles and buds preferentially from lipid raft domains. To extend these analyses, the relationship between the kinetics of viral protein dissociation from DRMs and incorporation into virus particles was determined, while the importance of NDV assembly and release at these domains was explored by disrupting lipid rafts.

Kinetics of viral protein dissociation from DRMs and incorporation into virions. If NDV is assembled and released preferentially from lipid raft domains, then there should be an inverse kinetic relationship between the association of viral proteins with DRMs and with virions released from cells, i.e., pulse-labeled DRM-associated viral proteins should decrease during a nonradioactive chase as these proteins are packaged into virus particles. However, for such an analysis to be meaningful, the assembly and release of virions must be very efficient. Indeed, the release of NDV from avian cells, the natural host of the virus, is extremely efficient. Based on the incorporation of pulse-labeled M protein into virions, the efficiency of NDV release is 90% for avian cells (Fig. 2) (H. Pantua and T. G. Morrison, unpublished observations).

In addition, an accurate kinetic analysis of the roles of lipid rafts in NDV assembly requires inclusion of all forms of DRMs. For the studies described here, a novel class of high-density DRMs, DRM-H, associated with the cortical cytoskeleton was included (30). Many studies that include DRM isolation do not utilize conditions that would clearly separate this fraction from the detergent-soluble fraction of cells, which may lead to significant underrepresentation of the amount of each viral protein associated with DRMs. The inclusion of DRM-H is also particularly important given that the actin cytoskeleton has been implicated in paramyxovirus assembly and that actin is incorporated into paramyxovirus particles (20, 33, 47). In addition, the importance of this cell fraction is underscored by the finding that the majority of DRM-associated viral NP and M proteins and a significant amount of HN protein were associated with DRM-H.

Using NDV-infected avian cells, significant amounts of pulse-labeled NP, F, and HN proteins were associated with DRMs after a short nonradioactive chase, and the loss of this material with longer chases was mirrored by the incorporation of these radiolabeled viral proteins into virus particles. Indeed, the amounts of NP, F, and HN proteins in DRMs were quantitatively recovered in virus at late chase times, while the pools of detergent-soluble viral proteins remained relatively constant during the nonradioactive chases. This result is consistent with the proposal that lipid rafts, as defined by DRMs, are the assembly sites of released NDV particles and that non-lipid-raft-associated viral proteins are not directly involved in virus release.

However, in contrast, the DRM association of the M protein was minimal after a short nonradioactive chase (20% of the total radiolabeled M protein), and this material decreased to undetectable levels with longer chases. In addition, the level of pulse-labeled detergent-soluble M protein declined with longer chase times and was quantitatively recovered in virus particles. The low levels of M protein detected in DRMs may reflect an association with lipid rafts that is disrupted by the concentration of Triton X-100 used here. Indeed, Ali and Nayak (2) reported that the M protein of Sendai virus was dissociated from DRMs by 1% Triton X-100 but could be detected with DRMs when lower Triton X-100 concentrations were used during DRM isolation. Alternatively, the results reported here may reflect a very transient association of the M protein with lipid rafts. Paramyxovirus M proteins have been shown to have a pivotal role in virus release (reviewed in reference 46). Indeed, the M protein is both necessary and sufficient for the release of NDV-like particles (33a), and this release is extremely efficient, with 80 to 90% of pulse-labeled M protein released as virus-like particles. Given this result, it is possible that when the M protein associates with virion assembly sites, it immediately induces the release of the virion. In this case, the M protein would not be detected in significant amounts in DRMs since it would be associated only transiently with this cell fraction. The M protein in detergent-soluble fractions of the cell would therefore decrease as this pool of molecules bound assembly sites and then exited the cell in virus particles.

The finding that DRM-associated NP and M proteins were present primarily in DRM-H suggests that assembly sites may be in or adjacent to lipid raft domains that are linked to the cortical cytoskeleton. The cortical cytoskeleton is a meshwork of actin underlying the plasma membrane, which is often linked to the plasma membrane by interactions with lipid raft-associated proteins (43). Since lipid rafts serve as sites of dynamic signaling events (42), rearrangements of proximal components of the cortical cytoskeleton often occur (13, 15). Further support of the possible role of the actin cytoskeleton in paramyxovirus assembly and release is found by the interaction among many paramyxovirus M proteins with actin (9) and the

ability of drugs affecting actin filaments to alter the release of some paramyxoviruses (5, 28, 45). Thus, the association of viral proteins with DRM-H is consistent with an involvement of the actin cytoskeleton in NDV assembly. Virus assembly and release from these domains may be facilitated by dynamic remodeling of the cortical cytoskeleton in these raft domains.

Similar to the results reported here, Manie et al. (22) showed that a fraction of pulse-labeled measles viral proteins were found in DRMs of infected cells. This material disappeared with long chases, although it was not determined if this material could be recovered in released virus. However, in contrast to the results presented here, most of the radiolabeled measles viral proteins remained in the detergent-soluble fraction of cells throughout the chase. It is possible that a significant fraction of this material was associated with DRM-H or that the efficiency of virus release was very low.

Effects of disruption of lipid rafts on release of infectious NDV. While the kinetics of viral protein dissociation from DRMs and release into virions strongly supports the idea that NDV assembly occurs in lipid raft domains, these results do not address the functional significance of lipid rafts as assembly sites. To explore the importance of lipid raft domains in assembly and release, lipid rafts were disrupted by the combined use of lovastatin, which inhibits the synthesis of endogenous cholesterol (16), and methyl-β-cyclodextrin, which extracts cholesterol from cellular membranes (17, 40, 42). Hao et al. (11) reported that mβCD-induced cholesterol depletion of several different cell types resulted in the formation in the plasma membrane of large, micrometer-sized liquid-ordered (raft-like) domains distinct from the surrounding liquid-disordered (nonraft) membrane. These results indicate that a reduction of cholesterol levels in the plasma membrane induces significant reorganization of plasma membrane lipids and coalescence of remaining liquid-ordered domains. Indeed, cholesterol extraction of avian cells resulted in large GM1-enriched domains, in stark contrast to a more uniform distribution of small punctate regions of GM1-positive domains in untreated cells. These observations suggest that in avian cells, there is also a reorganization of remaining liquid-ordered domains after cholesterol extraction. Kwik et al. (18) reported that cholesterol extraction results in reorganization of the actin cytoskeleton, resulting in a restriction in the lateral mobility of plasma membrane proteins. Given the connections between lipid rafts and the cortical cytoskeleton, it is not surprising that the cytoskeleton should be affected by rearrangement of liquid-ordered lipid raft domains at the cell surface. Indeed, the distribution of filamentous actin in cholesterol-extracted avian cells was significantly altered.

Following depletion of cholesterol from infected cell membranes, there was a reduction in DRM associations with both caveolin and actin, indicating that the protocols effectively removed cholesterol and altered the properties of lipid rafts. The association of viral proteins with DRMs was also significantly reduced. Surprisingly, virus particle release from cholesterol-depleted cells was not inhibited. Rather, particle release was somewhat stimulated, indicating that release is not strictly dependent upon the proper organization of lipid raft domains. However, the particles that were released were abnormal, displaying very heterogeneous densities and increased levels of NP relative to other virion components. Most interestingly, the infectivity of these particles, either normalized to numbers of virus-producing cells or normalized to NP protein content, was significantly reduced. In contrast, Pickl et al. (34) reported a reduction in Moloney murine leukemia virus particle production as well as particle infectivity upon treatment of virus-producing cells with mβCD.

The reduced infectivity of the NDV particles was not likely due directly to their decreased content of cholesterol, since extraction of cholesterol from intact, infectious virus had no effect on the infectivity of these particles. Furthermore, the virus particles released from cholesterol-depleted cells were all associated with lipids, as indicated by their flotation into sucrose gradients and by the resistance of NP and M proteins to protease digestion.

There are several possible explanations for the reduction in infectivity of these particles. The heterogeneous densities of the particles suggested significant alterations in protein-to-lipid ratios for a majority of the released particles. Furthermore, the particles that were heavier or lighter than infectious NDV particles released from untreated cells had reduced levels of glycoproteins. These particles would be unable to attach and fuse upon encountering a permissive cell, which could account for their reduced infectivity. However, the particles released from cholesterol-extracted cells with normal NDV particle densities had levels of glycoproteins comparable to those in particles released from untreated cells. These particles also had significantly diminished infectivity, indicating that the loss of infectivity cannot be explained by a loss of glycoproteins. These normal-density particles did, however, contain an increased amount of NP relative to glycoprotein, indicating a structural abnormality.

It is possible that lipid rafts and their underlying cortical cytoskeleton provide a framework for specific and ordered viral protein-protein interactions required for proper assembly. These domains may also contain host cell components required for virus assembly. Disruption or disordering of these domains upon extraction of cholesterol would therefore result in disordered virus assembly and subsequent release of particles with abnormal viral protein ratios and, perhaps, abnormal viral protein interactions.

It was recently reported that lipid raft domains have no role in the assembly of Sendai virus (10). However, as noted in the report, the assembly and release of Sendai virus are extremely inefficient in the cell type used, thereby making this investigation of the precursors to virus assembly and release problematic. The authors also used mβCD to extract cellular cholesterol and to perturb membrane lipid rafts. However, their conditions did not disrupt lipid raft domains since viral proteins remained associated with DRMs. They did note a slight reduction in the infectivity of particles released from mβCD-treated cells, a result consistent with the data presented here.

In summary, the results presented here demonstrate that lipid raft domains are the preferential site of NDV assembly and release. Furthermore, the integrity of these domains is important in the ordered assembly and release of infectious progeny NDV particles. The results also demonstrate the involvement of a novel subset of lipid rafts, those associated with the cortical cytoskeleton, in NDV assembly and release and further implicate the actin cytoskeleton in this step of infection. These results have implications on vaccine design and the development of antiviral agents. Understanding how viral pro-

teins associate with membrane lipid rafts and the importance of these domains in the organization of a particle could provide the basis for targeting foreign glycoproteins to these assembly sites for incorporation into budding NDV-based particles, thereby generating multivalent vaccines. Also, the perturbation of membrane lipid rafts by small molecules could provide a means for creating disordered virion assembly on infected cell surfaces, thereby inducing the release of noninfectious particles.

ACKNOWLEDGMENTS

We thank Gregory Hendricks (University of Massachusetts Medical School Core Electron Microscopy Facility) for electron microscopy of virus particles.

This work was supported by a grant from the National Institutes of Health (AI30572).

REFERENCES

1. **Ali, A., R. T. Avalos, E. Ponimaskin, and D. P. Nayak.** 2000. Influenza virus assembly: effect of influenza virus glycoproteins on the membrane association of M1 protein. J. Virol. **74:**8709–8719.
2. **Ali, A., and D. P. Nayak.** 2000. Assembly of Sendai virus: M protein interacts with F and HN proteins and with the cytoplasmic tail and transmembrane domain of F protein. Virology **276:**289–303.
3. **Barman, S., and D. P. Nayak.** 2000. Analysis of the transmembrane domain of influenza virus neuraminidase, a type II transmembrane glycoprotein, for apical sorting and raft association. J. Virol. **74:**6538–6545.
4. **Brown, G., J. Aitken, H. W. Rixon, and R. J. Sugrue.** 2002. Caveolin-1 is incorporated into mature respiratory syncytial virus particles during virus assembly on the surface of virus-infected cells. J. Gen. Virol. **83:**611–621.
5. **Burke, E., L. Dupuy, C. Wall, and S. Barik.** 1998. Role of cellular actin in the gene expression and morphogenesis of human respiratory syncytial virus. Virology **252:**137–148.
6. **Dolganiuc, V., L. McGinnes, E. J. Luna, and T. G. Morrison.** 2003. Role of the cytoplasmic domain of the Newcastle disease virus fusion protein in association with lipid rafts. J. Virol. **77:**12968–12979.
7. **Faaberg, K. S., and M. E. Peeples.** 1988. Strain variation and nuclear association of Newcastle disease virus matrix protein. J. Virol. **62:**586–593.
8. **Fenton, R. G., H. F. Kung, D. L. Longo, and M. R. Smith.** 1992. Regulation of intracellular actin polymerization by prenylated cellular proteins. J. Cell Biol. **117:**347–356.
9. **Giuffre, R. M., D. R. Tovell, C. M. Kay, and D. L. Tyrrell.** 1982. Evidence for an interaction between the membrane protein of a paramyxovirus and actin. J. Virol. **42:**963–968.
10. **Gosselin-Grenet, A. S., G. Mottet-Osman, and L. Roux.** 2006. From assembly to virus particle budding: pertinence of the detergent resistant membranes. Virology **344:**296–303.
11. **Hao, M., S. Mukherjee, and F. R. Maxfield.** 2001. Cholesterol depletion induces large scale domain segregation in living cell membranes. Proc. Natl. Acad. Sci. USA **98:**13072–13077.
12. **Harder, T., P. Scheiffele, P. Verkade, and K. Simons.** 1998. Lipid domain structure of the plasma membrane revealed by patching of membrane components. J. Cell Biol. **141:**929–942.
13. **Harder, T., and K. Simons.** 1999. Clusters of glycolipid and glycosylphosphatidylinositol-anchored proteins in lymphoid cells: accumulation of actin regulated by local tyrosine phosphorylation. Eur. J. Immunol. **29:**556–562.
14. **Henderson, G., J. Murray, and R. P. Yeo.** 2002. Sorting of the respiratory syncytial virus matrix protein into detergent-resistant structures is dependent on cell-surface expression of the glycoproteins. Virology **300:**244–254.
15. **Holowka, D., E. D. Sheets, and B. Baird.** 2000. Interactions between Fc(epsilon)RI and lipid raft components are regulated by the actin cytoskeleton. J. Cell Sci. **113:**1009–1019.
16. **Keller, P., and K. Simons.** 1998. Cholesterol is required for surface transport of influenza virus hemagglutinin. J. Cell Biol. **140:**1357–1367.
17. **Kilsdonk, E. P., P. G. Yancey, G. W. Stoudt, F. W. Bangerter, W. J. Johnson, M. C. Phillips, and G. H. Rothblat.** 1995. Cellular cholesterol efflux mediated by cyclodextrins. J. Biol. Chem. **270:**17250–17256.
18. **Kwik, J., S. Boyle, D. Fooksman, L. Margolis, M. P. Sheetz, and M. Edidin.** 2003. Membrane cholesterol, lateral mobility, and the phosphatidylinositol 4,5-bisphosphate-dependent organization of cell actin. Proc. Natl. Acad. Sci. USA **100:**13964–13969.
19. **Lamb, R. A., and D. Kolakofsky.** 2001. Paramyxoviridae: the viruses and their replication. *In* D. M. Knipe, P. M. Howley, D. E. Griffin, R. A. Lamb, M. A. Martin, B. Roizman, and S. E. Straus (ed.), Fields virology. Lippincott Williams & Wilkins, Philadelphia, Pa.
20. **Lamb, R. A., B. W. Mahy, and P. W. Choppin.** 1976. The synthesis of Sendai virus polypeptides in infected cells. Virology **69:**116–131.
21. **Li, M., C. Yang, S. Tong, A. Weidmann, and R. W. Compans.** 2002. Palmitoylation of the murine leukemia virus envelope protein is critical for lipid raft association and surface expression. J. Virol. **76:**11845–11852.
22. **Manie, S. N., S. Debreyne, S. Vincent, and D. Gerlier.** 2000. Measles virus structural components are enriched into lipid raft microdomains: a potential cellular location for virus assembly. J. Virol. **74:**305–311.
23. **McGinnes, L. W., K. Gravel, and T. G. Morrison.** 2002. Newcastle disease virus HN protein alters the conformation of the F protein at cell surfaces. J. Virol. **76:**12622–12633.
24. **McGinnes, L. W., and T. G. Morrison.** 2006. Inhibition of receptor binding stabilizes Newcastle disease virus HN and F protein-containing complexes. J. Virol. **80:**2894–2903.
25. **McGinnes, L. W., H. Pantua, and T. G. Morrison.** 2006. Newcastle disease virus: propagation, quantification, and storage, p. 15F.2.1–15F.2.18. *In* R. Coico, T. Kowalik, J. Quarles, B. Stevenson, and R. Taylor (ed.), Current protocols in microbiology. John Wiley & Sons, Inc., New York, N.Y.
26. **McGinnes, L. W., J. N. Reitter, K. Gravel, and T. G. Morrison.** 2003. Evidence for mixed membrane topology of the Newcastle disease virus fusion protein. J. Virol. **77:**1951–1963.
27. **Melkonian, K. A., A. G. Ostermeyer, J. Z. Chen, M. G. Roth, and D. A. Brown.** 1999. Role of lipid modifications in targeting proteins to detergent-resistant membrane rafts. Many raft proteins are acylated, while few are prenylated. J. Biol. Chem. **274:**3910–3917.
28. **Morrison, T. G., and L. J. McGinnes.** 1985. Cytochalasin D accelerates the release of Newcastle disease virus from infected cells. Virus Res. **4:**93–106.
29. **Morrison, T. G., M. E. Peeples, and L. W. McGinnes.** 1987. Conformational change in a viral glycoprotein during maturation due to disulfide bond disruption. Proc. Natl. Acad. Sci. USA **84:**1020–1024.
30. **Nebl, T., K. N. Pestonjamasp, J. D. Leszyk, J. L. Crowley, S. W. Oh, and E. J. Luna.** 2002. Proteomic analysis of a detergent-resistant membrane skeleton from neutrophil plasma membranes. J. Biol. Chem. **277:**43399–43409.
31. **Nguyen, D. H., and J. E. Hildreth.** 2000. Evidence for budding of human immunodeficiency virus type 1 selectively from glycolipid-enriched membrane lipid rafts. J. Virol. **74:**3264–3272.
32. **Ono, A., and E. O. Freed.** 2005. Role of lipid rafts in virus replication. Adv. Virus Res. **64:**311–358.
33. **Orvell, C.** 1978. Structural polypeptides of mumps virus. J. Gen. Virol. **41:**527–539.

33a. **Pantua, H., and T. G. Morrison.** J. Virol., in press.

34. **Pickl, W. F., F. X. Pimentel-Muinos, and B. Seed.** 2001. Lipid rafts and pseudotyping. J. Virol. **75:**7175–7183.
35. **Pornillos, O., J. E. Garrus, and W. I. Sundquist.** 2002. Mechanisms of enveloped RNA virus budding. Trends Cell Biol. **12:**569–579.
36. **Rixon, H. W., G. Brown, J. Aitken, T. McDonald, S. Graham, and R. J. Sugrue.** 2004. The small hydrophobic (SH) protein accumulates within lipid-raft structures of the Golgi complex during respiratory syncytial virus infection. J. Gen. Virol. **85:**1153–1165.
37. **Saifuddin, M., C. J. Parker, M. E. Peeples, M. K. Gorny, S. Zolla-Pazner, M. Ghassemi, I. A. Rooney, J. P. Atkinson, and G. T. Spear.** 1995. Role of virion-associated glycosylphosphatidylinositol-linked proteins CD55 and CD59 in complement resistance of cell line-derived and primary isolates of HIV-1. J. Exp. Med. **182:**501–509.
38. **Salzer, U., and R. Prohaska.** 2001. Stomatin, flotillin-1, and flotillin-2 are major integral proteins of erythrocyte lipid rafts. Blood **97:**1141–1143.
39. **Sanderson, C. M., R. Avalos, A. Kundu, and D. P. Nayak.** 1995. Interaction of Sendai viral F, HN, and M proteins with host cytoskeletal and lipid components in Sendai virus-infected BHK cells. Virology **209:**701–707.
40. **Scheiffele, P., M. G. Roth, and K. Simons.** 1997. Interaction of influenza virus haemagglutinin with sphingolipid-cholesterol membrane domains via its transmembrane domain. EMBO J. **16:**5501–5508.
41. **Schmitt, A. P., and R. A. Lamb.** 2004. Escaping from the cell: assembly and budding of negative-strand RNA viruses. Curr. Top. Microbiol. Immunol. **283:**145–196.
42. **Simons, K., and D. Toomre.** 2000. Lipid rafts and signal transduction. Nat. Rev. Mol. Cell Biol. **1:**31–39.
43. **Simpson-Holley, M., D. Ellis, D. Fisher, D. Elton, J. McCauley, and P. Digard.** 2002. A functional link between the actin cytoskeleton and lipid rafts during budding of filamentous influenza virions. Virology **301:**212–225.
44. **Skibbens, J. E., M. G. Roth, and K. S. Matlin.** 1989. Differential extractability of influenza virus hemagglutinin during intracellular transport in polarized epithelial cells and nonpolar fibroblasts. J. Cell Biol. **108:**821–832.
45. **Stallcup, K. C., C. S. Raine, and B. N. Fields.** 1983. Cytochalasin B inhibits the maturation of measles virus. Virology **124:**59–74.
46. **Takimoto, T., and A. Portner.** 2004. Molecular mechanism of paramyxovirus budding. Virus Res. **106:**133–145.
47. **Tyrrell, D. L., and E. Norrby.** 1978. Structural polypeptides of measles virus. J. Gen. Virol. **39:**219–229.
48. **Vincent, S., D. Gerlier, and S. N. Manie.** 2000. Measles virus assembly within membrane rafts. J. Virol. **74:**9911–9915.
49. **Wang, C., G. Raghu, T. Morrison, and M. E. Peeples.** 1992. Intracellular processing of the paramyxovirus F protein: critical role of the predicted amphipathic alpha helix adjacent to the fusion domain. J. Virol. **66:**4161–4169.